Desalination and Water Treatment
www.deswater.com

doi: 10.5004/dwt.2018.22953

125 (2018) 81–92
September

Adsorption and kinetic studies of hexavalent chromium by dehydrated *Scrophularia striata* stems from aqueous solutions

Mansooreh Dehghani, Majid Nozari, Iman Golkari, Nasrin Rostami, Marziyeh Ansari Shiri*

Research Center for Health Sciences, Department of Environmental Health, School of Health, Shiraz University of Medical Sciences, Shiraz, Iran, email: mdehghany@sums.ac.ir (M. Dehghani), majidnozari2018@gmail.com (M. Nozari), imangolkari110@gmail.com (I. Golkari), nasrinrostami676@gmail.com (N. Rostami), Tel./Fax +98-711-7260225, email:marziyehansari566@gmail.com (M.A. Shiri)

Received 21 March 2018; Accepted 14 August 2018

ABSTRACT

The unregulated discharge of heavy metals into the environment from industrial activities is an important threat to the environment. In this study, the adsorption of Cr(VI) from aqueous solution onto dehydrated *Scrophularia striata* stems (DSSS) was studied. The effects of pH, the adsorbent dosage, the initial Cr(VI) concentration, and the reaction time on the adsorption efficiency were investigated. The Brunauer–Emmett–Teller (BET), Fourier transform infrared (FTIR), and SEM-energy dispersive X-ray (EDX) analyses were performed to assess the pores volume, chemical form, and surface morphology of the DSSS, respectively. Moreover, the kinetics and thermodynamics of Cr(VI) adsorption were theoretically interpreted using different models. The adsorption efficiency of Cr(VI) decreased as the pH and initial Cr(VI) concentration increased. Conversely, the adsorption efficiency increased as the adsorbent dose and reaction time increased. The kinetic processes of Cr(VI) adsorption were tested by applying the pseudo-first-order, pseudo-second-order, and Elovich models. The pseudo-first-order kinetic model for Cr(VI) adsorption fitted well. The Langmuir isotherm provided the best correlation for the adsorption of Cr(VI) onto DSSS. Accordingly, it is concluded that DSSS can be used as an affordable, appropriate, and environmentally friendly adsorbent for Cr(VI) adsorption from aqueous solutions.

Keywords: Kinetic; Isotherm; Adsorption; Cr(VI); Scrophularia striata

1. Introduction

Environmental pollution by industrial wastes is an important concern due to toxicity and the danger it has for human health and the environment [1]. Heavy metals are produced in large amounts during industrial activities and contaminate the environment. Metal ions are non-biodegradable, and many are soluble in aqueous media and easily available for living organisms. Heavy metals account for a number of disorders in plants and animals, and their removal from aqueous media is an important and challenging task [2].

Cr(VI) is one of the most hazardous pollutants due to its small size, stability, and solubility in water. Cr(VI) causes cancer in the digestive tract and lungs as well as a number of other diseases [3]. Chromium exists in aqueous media in two oxidation states: Cr(VI) and Cr(III). The toxicity of chromium depends upon its oxidation state. In solution, Cr(VI) exists in various forms depending upon the pH, such as chromate ($Cr_2O_4^{2-}$), hydrochromate ($HCrO^{4-}$), and dichromate ($Cr_2O_7^{2-}$) [4]. Chromium compounds (chromate (CrO_4^{2-}) and dichromate ($Cr_2O_7^{2-}$)) are frequently water soluble and are highly toxic to humans. They cause serious health hazards, such as allergic reactions, respiratory disorders, diarrhea, and stomach and intestinal bleeding [5]. The recommended daily dietary intake (DDI) of chromium for humans is 50–200 μg/d [2]. Chromium compounds are major environmental pollutants, and their existence in water and wastewater has caused many problems. Various industries, such as metal mines, refineries, chemical fertilizer–producing factories, dyeing, tanning, and textile manufacturing are involved in the

*Corresponding author.

generation of wastewater containing chromium [5]. Several technologies have been applied to remove Cr(VI) from aqueous solutions including precipitation, reverse osmosis, ion exchange, filtration, sand filtration, chemical reduction/oxidation, and electrochemical deposition [6]. However, these methods have limitations due to the production of secondary wastes, the large quantity of slug formation, and high operational costs [2]. Currently, adsorption techniques receive more attention because of their low-cost, high effectiveness, and simplicity of applying for decolorization [7,8].

Cr(VI) has got unique properties of corrosion resistance, hardness and colour and therefore finds large number of applications in industries like chrome-plating, automobiles, steel and alloys, paints, leather tanning and ammunition factories [9]. Consequently, these industries discharge large quantities of chromium-containing effluents. Since chromium is a known mutagen and carcinogen [10], the prevalent pollution laws in most countries require its complete elimination from waste streams before emancipation. The most commonly used method for chromium removal method is reduction followed by chemical precipitation [11]. However, this process has many disadvantages like high installation costs, high energy-intensive, consumption of large quantities of chemicals, and difficulty of handling the later produced solid waste; hence, it is economically unattractive. Therefore, it is necessary to look for a new practical, economic, efficient and sustainable alternative for the management of chromium-bearing industrial effluents. Agricultural by-products including wood, corn, pulp, rice husks, coal, paper waste, sewage sludge, sawdust, charcoal, bituminous coal, straw, and wood are low-cost adsorbents that are effective and abundant in nature. However, the disposal of some of these products is often difficult [12]. The *Scrophulariaceae* is a large angiosperm family, which is widely distributed in deciduous and coniferous forests of Central Europe, Central Asia, and North America, especially in the Mediterranean area [13]. To date, no study has explored the removal of Cr(VI) from aqueous solution using adsorption on dehydrated *Scrophularia striata* stems (DSSS). The present study aimed to investigate the efficiency of DSSS as a natural, cheap, and available means for adsorption of Cr(VI) from aqueous solutions.

2. Experimental

2.1. Preparation of adsorbent

Scrophilaria striata (a schematic presented in Fig. 1) was gathered from the Zagros Mountains in the beginning of summer in 2016. Stem parts of the plant were separated, shredded, and washed with distilled water. Subsequently, they were placed in an oven (Model DHG-9000, Zhengzhou Protech Technology Co, Ltd, China) at 88 for two hours to dehydrate fully. Later, the dehydrated stems were pulverized and rinsed with hydrochloric acid (10% solution) to remove the dye developed in the powdered stems, and then washed with distilled water to eliminate the remaining acid. Lastly, the powdered stems were passed through a 60–100 mesh sieve to generate a homogeneous adsorbent.

Fig. 1. A schematic image of *Scrophilaria striata*.

2.2. Preparation of Cr(VI) solution

A solution of Cr(VI) (500 mg/L) was prepared by adding potassium dichromate ($K_2Cr_2O_7$) to distilled water. Aqueous solutions of H_2SO_4 and NaOH were used to adjust the pH, the value of which was measured by an electrode method (Metrohm, Switzerland) [14]. All the needed chemical materials were purchased from Merck (Germany).

2.3. Adsorption studies

A bench-scale experiment was performed on a laboratory scale. The specific amount of the adsorbent and a certain amount of pollutants were in contact at different pH values. For this purpose, a shaker (Model E5650 Digital Benchtop Reciprocal Shaker, Eberbach, Germany) with a mixing speed of 25 rpm was used. The samples were collected after the completion of the reaction time. Adsorbent particles were isolated from the solution through centrifugation at 45,000 rpm. The concentration of Cr(VI) was measured by a 311B method, using 1–5, Diphenylcarbazide reagent and spectrophotometer (Plus UV/Visible SP–3000, Japan) at a wavelength of 540 nm [15]. Cr(VI) adsorption efficiency (%) and adsorption capacity of the adsorbent were calculated, using the Eqs. (1) and (2) [16,17]:

$$R(\%) = \frac{C_0 - C_e}{C_0} \times 100 \quad (1)$$

Table 1
The essential physical and chemical properties of adsorbate

Molecular weight	52 g/mol
Boiling point	2642°C
Melting point	1900°C
Specific gravity	7.14
Color	Silver-White to Grey
Odor	Odorless
Taste	Not available
Critical temperature	Not available
Volatility	Not available
Solubility	Just soluble in acids (except Nitric), and strong alkalies

$$q_e = \frac{(C_0 - C_e) \times V}{M} \quad (2)$$

where R (%) is the efficiency of removal, q_e is the number of metal ions adsorbed onto the unit mass of the adsorbent (mg/g), C_0 and C_e are the concentration of metal ions before and after adsorption (mg/L), V is the volume of the aqueous phase (L), and M is the mass of the adsorbent (g).

2.4. Adsorption parameters

The effects of various operating parameters such as Cr(VI) initial concentration (2–10 mg/L), pH (2–10), adsorbent dose (0.1–2 g/100 mL), and reaction time (20–180 min) were investigated. Adsorption experiments for the effect of pH were directed using a solution containing 10 mg/L of Cr(VI) concentration with an adsorbent dosage of 2 g/100 mL and a reaction time of 60 min. The pH was fixed with a range of 2–10. The effect of adsorbent dosage on adsorption efficiency of Cr(VI) was experimented using Cr(VI) concentration of 10 mg/L, reaction time of 60 min and pH fixed to 2. The selected concentration range of the adsorbent was used from 0.1 to 2 g/100 mL. The effect of the differentiation of the initial concentration was investigated using a Cr(VI) initial concentration 2 to 10 mg/L, at pH 2, reaction time of 60 min and adsorbent dosage of 2 g/100 mL. The effect of reaction time on adsorption efficiency of Cr(VI) was experimented using Cr(VI) concentration of 2 mg/L, the adsorbent dosage of 2 g/100 mL, and pH fixed to 2, and the reaction time at a range of 20–180 min. All the investigations were carried out in triplicate to confirm the reproducibility of the experimental results.

2.5. Analysis

The textural characteristics of DSSS including specific surface area, total pore volume, and pore size distribution were obtained from N_2 adsorption/desorption data at 77K, using surface area analyzer with BEL sorp-mini II, Japan model. The surface area of the adsorbent was estimated by the BET equation. The total pore volume was calculated at relative pressure and $p\ p_0^{-1}$ of 0.99, and micropore volume was determined using the t-plot method. Mesopore volume can be calculated by deducting micropore volume from the total pore volume [18]. The porous properties of the prepared activated carbon are presented in Table 2 and the accuracy of the values is based on the apparatus accuracy. The surface morphology of the DSSS was visualized by using scanning electron microscopy with a VEGA II TESCAN, CZECH model. The qualitative elemental composition of the DSSS was determined by EDX spectroscopy with a VEGA II TESCAN, CZECH model. FTIR spectra of the DSSS were recorded before and after Cr(VI) ion adsorption in the frequency range of 400–4000 cm^{-1} by Shimadzu, FTIR1650 spectrophotometer, Japan.

Table 2
Characteristic of DSSS

Parameter	Value
BET surface area ($m^2\ g^{-1}$)	125.14
Total pore volume ($cm^3\ g^{-1}$)	0.2123
Micropore volume ($cm^3\ g^{-1}$)	0.1206
Mesoporosity (%)	48
Average pore diameter (nm)	6.5931

2.6. Adsorption kinetics

To analyze the adsorption kinetics of Cr(VI) by DSSS pseudo-first-order [7,19], we tested the pseudo-second-order [7] and Elovich model [20]. The kinetic parameters were analyzed in a batch adsorption experiment of 2–10 mg/L of Cr(VI) at pH 2. The reaction time ranged from 20–180 min and the adsorption efficiency of Cr(VI) was tacked during the study.

In the batch–reaction time experiment in which the adsorption quantity of Cr(VI) onto the adsorbent surface corresponds to the rate of Cr(VI) adsorbed from the solution phase, the pseudo-first-order equation is usually written as follows [7,19,21]:

$$\ln(q_e - q_t) = \ln q_e - K_1 t \quad (3)$$

where q_e and q_t are the adsorption efficiency (mg/g) of Cr(VI) at equilibrium and at a time t, respectively, and K_1 is the constant for pseudo-first-order adsorption (L/min).

The pseudo-second-order equation may be expressed as Eq. (4) to compute the efficiency of adsorption of Cr(VI) [7,21].

$$\frac{1}{q_t} = \frac{1}{K_2 q_e^2} + \frac{1}{q_e} t \quad (4)$$

where q_e and q_t are the adsorption efficiency (mg/g) of Cr(VI) at equilibrium and at a time t, respectively, and K_2 is the constant for pseudo-second-order adsorption (g/mg·min).

The equation of Elovich model is asserted as [20]:

$$q_t = \beta \ln(\alpha\beta) + \beta \ln t \quad (5)$$

where q_t is the adsorption efficiency (mg/g) of Cr(VI) at time t, α is the initial Cr(VI) concentration (mg/g·min) and β is desorption constant (g/mg) during an experiment. The constants can be computed from the slope and the intercept of the linear plot of q_t versus ln t. Eq. (5) was used to test the applicability of the Elovich equation to the kinetics of Cr(VI) adsorption onto the adsorbent.

2.7. Adsorption isotherms

Adsorption isotherm examines were conducted with different initial concentrations of Cr(VI) from 2 to 10 mg/L at pH 2. The reaction time ranged from 20 to 180 min, and the dosage of the adsorbent was 2 g/100 mL. In this work,

the Langmuir, Freundlich, and Temkin models [7] were used to describe the interaction between the adsorbent and Cr(VI). The correlation coefficient (R^2) was used to compute the best-fitted isotherm model.

The following equation (Eq. (6)) is expressed as Langmuir isotherm [7,22,23]:

$$\frac{C_e}{q_e} = \frac{1}{K_L qm} + \frac{C_e}{qm} \tag{6}$$

where q_m (mg/g) and K_L (L/mg) are the maximum adsorption efficiency and the dependency constant, respectively. The Langmuir isotherm has various limitations such as restricted places for the adsorption by developing monolayer adsorption on the adsorbent outside.

The Freundlich isotherm model is an empirical equation applied to describe various systems [7,21,23]. Freundlich adsorption isotherm is presented in Eq. (7):

$$\ln q_e = \ln K_f + \frac{1}{n} \ln C_e \tag{7}$$

where K_f ((mg/g)(mg/L)^n) and Freundlich constant (n) correspond to adsorption efficiency and adsorption intensity, respectively. K_f and n can be attained from the linear plot of log q_e against log C_e.

Temkin adsorption isotherm is written in the following equation [7]:

$$q_e = B \ln K_T + B \ln C_e \tag{8}$$

where K_T and B are the constant of Temkin isotherm (L/g), and the adsorption heat (J/mol), respectively.

2.8. Thermodynamic studies

The activation parameters give an insight if the adsorption process follows an activated complex before the final adsorption. The value of the activation energy, E_a, can be calculated via the Arrhenius equation in Eq. (9), using kinetic rate constants at various temperatures [11,24].

$$\ln k = \ln A \frac{E_a}{RT} \tag{9}$$

For E_a values between 5 and 20 kJ/mol, the predominant adsorption mechanism is physicorption, whereas for E_a values <40 kJ/mol, the adsorption is controlled by chemical reaction processes [25]. The activation energy (E_a = 22.7 kJ/mol) confirms the chemisorption nature of the adsorption process. On the other hand, the standard enthalpy of activation (ΔH*) and entropy of activation (ΔS*) can be computed using the Eyring equation in Eq. (10) and the free energy of activation (ΔG*) from Eq. (11) [23,26].

$$Ln\left(\frac{k}{T}\right) = Ln\frac{K_B}{h} + \frac{\Delta S^*}{R} - \frac{\Delta H^*}{T} \tag{10}$$

$$\Delta G^* = \Delta H^* - T\Delta S^* \tag{11}$$

The values for ΔG* (52.5, 54.7, and 55.6 kJ/mol) at different temperatures (298, 305, and 320 K) were positive, suggesting that adsorption requires energy to convert the reactants into products [25,26]. The computed ΔG* may also refer to the energy needed to overcome the activation energy and/or to form an activated complex, while ions were in the transition state for the adsorption process to proceed [27]. The positive value of ΔH* (2.8 kJ/mol) confirms the endothermic mechanism of activation [25,26]. The increasing kinetic rates at higher temperatures (Table 3) also validate the endothermic nature of the process. Similar findings were reported by others [28,29].

The negative value of ΔS* (–0.19 kJ/mol/K) indicates that Cr(VI) is associative and that an activated complex is formed between Cr(VI) and DSSS. Furthermore, it implies

Table 3
Kinetic parameter values for pseudo-first-order and pseudo-second-order models

Temp (K)	Initial Cr (VI)	Pseudo-first-order			Pseudo-second-order			
	Conc. (mg/L)	k_1 (×10^{-2} min^{-1})	$q_{t'}$ cal (×10^{-2} mg/g)	R^2	K_2 (×10^{-2} min^{-1})	$q_{t'}$ cal (×10^{-2} mg/g)	h (×10^{-3} mg/g. min)	R^2
298	2	3.11	1.13	0.936	4.85	2.21	2.34	0.898
	5	2.41	8.96	0.861	4.45	15.8	8.55	0.941
	10	1.65	6.35	0.459	4.63	13.22	8.62	0.973
305	2	2.87	1.52	0.879	4.72	5.71	17.28	0.989
	5	3.29	7.56	0.671	1.16	26.6	95.15	0.990
	10	1.41	5.03	0.922	1.33	62.7	57.52	0.993
320	2	2.13	0.63	0.734	8.84	17.55	59.85	0.997
	5	0.52	1.63	0.158	5.64	36.31	87.25	0.998
	10	–1.15	1.21	0.453	1.78	67.7	82.43	0.999

that no significant change in the internal structure of the adsorbent takes place during the adsorption [25,30,31].

2.9. Regeneration

Regeneration of the adsorbent, as well as recovery of the adsorbate material, is quite important. For this reason, the desorption studies were conducted using different desorbing agents like HNO_3, HCl, NH_4OH, and NaCl. The adsorbent loaded with Cr(VI) was placed in the desorbing medium and was constantly stirred on a rotatory shaker at 100 rpm for an hour at 303 K. Desorption ratio is given as the number of metal ions desorbed to the number of metal ions adsorbed multiplied by 100.

2.10. Statistical analysis

The relationship between the affecting parameters and the adsorption efficiency (%) was determined using multiple linear regression calculations. P value < 0.05 was considered statistically significant. SPSS statistical package, version 19.0, was used to analyze the data.

3. Result and discussion

3.1. Surface characterization

SEM image and EDX spectrum of DSSS before and after adsorption of Cr(VI) ions are shown in Figs. 2a and 2b, respectively. As shown in Fig. 2a, the surface of DSSS has an irregular surface containing pores with different sizes and shapes. As shown in Fig. 2b, some pores have been closed due to adsorbent surface converge by adsorbate. By comparing the EDX spectrum of Cr(VI) unloaded and loaded adsorbent, it can be concluded that Cr(VI) is adsorbed onto the DSSS. In this work, the FTIR spectra were obtained in order to analyze the mechanism of the Cr(VI) adsorption and identify functional groups on the surface of the prepared activated carbon. Fig. 3 shows the FTIR spectra of the adsorbent before and after Cr(VI) adsorption. The FTIR spectra bands indicate three major absorption bands including carboxyl, hydroxyl, and amino groups. The differences in the band intensity can be attributed to interaction of Cr(VI) ions with functional groups on the

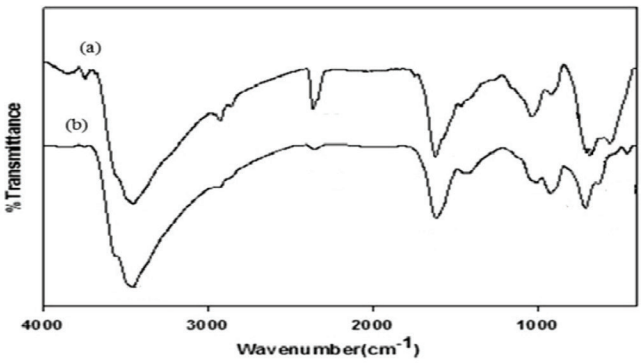

Fig. 3. FTIR spectra of the DSSS (a) without Cr(VI) adsorption and (b) with Cr(VI) adsorption.

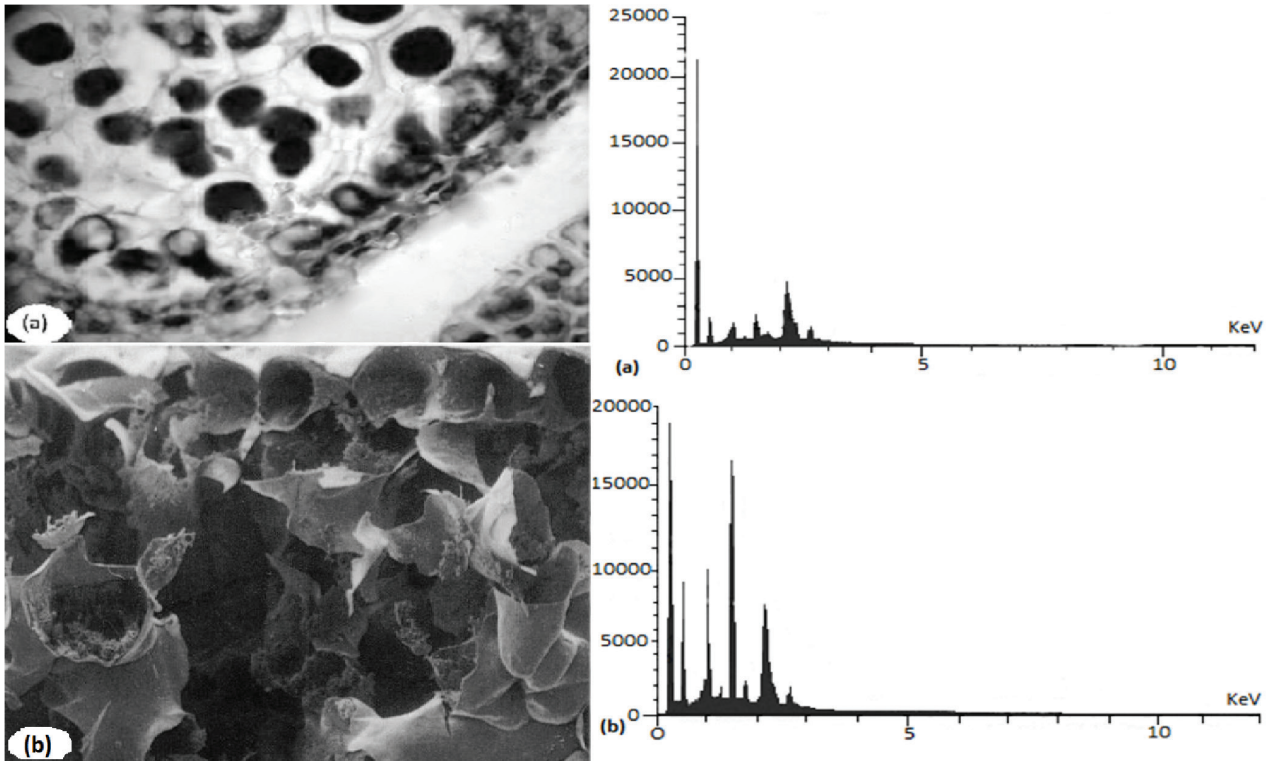

Fig. 2. SEM-EDX images of DSSS (a) before and (b) after adsorption of Cr(VI) ions.

adsorbent surface [32]. The broad absorption band at about 3456 cm^{-1} is attributed to the complexation between –OH groups which has been shifted to 3476 cm^{-1} after Cr(VI) adsorption [18]. The next shift observed at 1618 to 1612 cm^{-1} may be due to the complexation between Cr(VI) ions with carboxylic group (–C=O) [33]. According to FTIR analysis reported in the literature [34,35], the shift observed from 1004 to 1031 cm^{-1} is probably due to the interaction of nitrogen from amino group with Cr(VI). Doke and Khan used treated waste newspaper as a low-cost adsorbent [36]. They revealed that the most abundant functional groups found on the prepared activated carbon include aromatic (C–H), carboxylic acid (C–O, C=O, and O–H), carbonyl (C=O), alkane (C–H), and amine (N–H, C–N). On the other hand, since the paper mill sludge has a significant amount of phosphorus (shown in EDX analysis), this peak may be referred to the aliphatic P–O stretching [37] .

3.2. Effects of operating parameters

The pH of a solution is one of the most important parameters controlling the adsorption process, so it is necessary to measure it. The solution pH affects the surface charge of the adsorbent, the degree of the ionization, and specification of the adsorbate [38,39]. It is also a key factor in the adsorption of pollutants [40]. There is a strong effect of pH on the adsorption of heavy metals as a result of the surface change and the degree of ionization of the adsorbent [38].

As shown in Fig. 4, the adsorption efficiency of Cr(VI) extremely reduced as the pH increased from 2 to 10 (97.3% to 26.2%). In a study by Malkoc et al. [5], the sorption capacity of Cr(VI) at pH 2.0 by the waste pomace of an olive oil factory was 8.4 mg/g, which was reduced to 2.7 mg/g at pH 5.0. In studies conducted by Malkoc et al. [5] and Albadarin et al. [41], the maximum Cr(VI) adsorption was obtained at pH 2.0. According to a study carried out by Zhang et al. [15] on Cr(VI) adsorption of sulfonated lignite, the maximum adsorption of Cr(VI) ions occurred at high–acidity pH values because in the initial acid media, the chromium ions formed negatively charged hydrolyzed species. Also, a study by Hamidi et al. [17] showed that the removal of Cr(VI) was favored at a low pH. According to the regression analysis, there was a significant difference between pH and Cr(VI) adsorption efficiency ($p<0.005$). Other studies have reported opposite results compared to those found in the present study; that is, they reported that the adsorption efficiency of Cr(VI) increased with increasing pH [42,43].

One of the basic parameters in the adsorption process is the dose of the adsorbent used; as seen in Fig. 4, the adsorption efficiency of Cr(VI) (97.2%) extremely increased as the adsorbent dose increased up to 1g per 100 mL; after that, it slowly enhanced. With the adsorption efficiency of Cr(VI) for 0.1 to 2.0 g per 100 mL, the dose of the adsorbent was 86.5%, 87.2%, 92.5%, 97.2, 97.8%, 98%, and 98.3%, respectively (Fig. 4). According to regression analysis, there was a significant difference between the adsorbent dose and Cr(VI) adsorption efficiency ($p<0.005$). The present

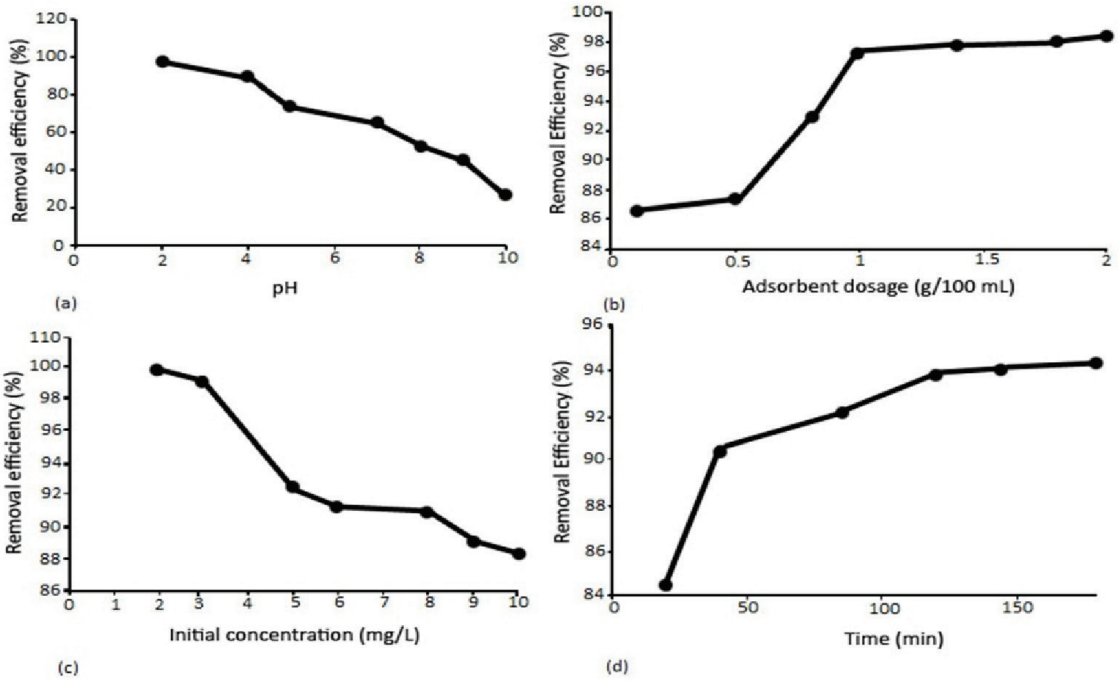

Fig. 4. (a); Adsorption efficiency of Cr(VI) at different pH levels (the initial concentration of Cr(VI): 10 mg/L; adsorbent dose: 2 g/100; reaction time: 60 min) (b); Adsorption efficiency of Cr(VI) at different adsorbent dosages (pH = 2; the initial concentration of Cr(VI): 10 mg/L; reaction time: 60 min) (c); Adsorption efficiency of Cr(VI) at different initial concentrations (pH = 2; adsorbent dose: 2 g/100 mL; reaction time: 60 min) (d); Adsorption efficiency of Cr(VI) at different reaction times (pH = 2; adsorbent dose: 2 g/100 mL; the initial concentration of Cr(VI): 2 mg/L).

study results showed that the efficiency of the adsorption enhanced with the increase in the adsorbent dose. The enhancement in adsorption efficiency of Cr(VI) may be related to the increase in the dose of the adsorbent which led to an increase in the number of active adsorption sites. In reality, by enhancing the dose of the adsorbent, many sites of adsorption will get free and cooperate in adsorption. However, an increase in the adsorbent dose will lead to unsaturated sorption sites, and the metals ions are inadequate to cover all the redeemable sites [44]. In Malkoc et al.'s [5] study, the removal of chromium by waste pomace of an olive oil factory (WPOOF) at different adsorbent doses (5–15 g/L) for the Cr(VI) concentration of 100 mg/L was investigated. The results showed that the percentage of the removal of Cr(VI) increased rapidly with the increase in the dose of WPOOF due to the greater availability of the adsorbent. In Bhattacharya et al.'s [45] study, it was indicated that the Cr(VI) removal efficiency enhanced with the increase in the concentration of the adsorbent.

One of the most important factors affecting the adsorption process is the initial concentration of the pollutant. Fig. 4 demonstrates the effect of initial Cr(VI) concentration on the efficiency of adsorption. The adsorption efficiency of Cr(VI) at the initial concentration of 2, 3, 5, 6, 8, 9 and 10 mg/L was 99.7%, 99.2%, 92.5%, 91.2%, 90.8%, 89%, and 88.2%, respectively (Fig. 4). Regression analysis showed that there was a significant difference between the initial concentration and Cr(VI) adsorption efficiency ($p < 0.005$). The Cr(VI) adsorption efficiency reduced with the enhancement of the Cr(VI) initial concentration, which may be associated with the inadequacy of free adsorption sites and the lack of emptiness in active sites. Indeed, the Cr(VI) initial concentration, due to the mass transfer resistance between the solid and liquid phases, produces an extremely driving force. At low metal ion/adsorbent ratios, metal ion adsorption involves higher energy sites. As the metal ion/adsorbent ratio increases, the higher energy sites are saturated, and adsorption begins on lower energy sites, resulting in a decrease in the adsorption efficiency [46]. Furthermore, other studies have reported similar results [5, 45]. However, the results of other studies are not consistent with those of this study [47,48].

As seen in Fig. 4, the efficiency of Cr(VI) adsorption increased hastily with the increase in the reaction time to 40 min. A more increase in reaction time had a trivial effect on the removal efficiency. The reaction time of 180 min was the maximum adsorption efficiency of Cr(VI). Regression analysis also showed that there was a significant difference between the reaction time and Cr(VI) adsorption efficiency ($p < 0.005$). Bhattacharya et al. [45] reported that with an increase in the reaction time from 0.5 to 2 h, the efficiency of the removal of Cr(VI) increased significantly. Also, the results of the study conducted by Zhang et al. [15] indicated that with the increase in the reaction time from 10 to 120 min, the adsorption efficiency of Cr(VI) was increased. The quality of the adsorbent and its adequate sorption sites influenced the reaction time required to reach the equilibrium [24]. However, a report was not in the same line with the present results [17].

3.3. Adsorption kinetic

Adsorption kinetic studies are very important for evaluating the feasibility of pollutant retention by solid media, and understanding how fast an adsorption process reaches the equilibrium and the mechanism involved in the reaction; for analysis of the adsorption kinetics of Cr(VI) by DSSS, the kinetic models of pseudo-first-order, pseudo-second-order and Elovich were investigated. In this study, the Cr(VI) adsorption kinetic models onto DSSS were analyzed with initial Cr(VI) concentration of 2, 3, 5, 6, 8, 9, and 10 mg/L. The values of K_1, K_2, α, β, and q_e were calculated from three linear kinetic models, and their corresponding correlation coefficients (R^2) are presented in Table 4. The constant rate of K_2 and equilibrium concentration of Cr(VI) q_e can be calculated from the slope and intercept of the plot (Fig. 7). The correlation coefficients (R^2) for the pseudo-first-order, pseudo-second-order, and Elovich kinetic models in different concentrations were at ranges of 0.855–0.966, 0.822–0.948 and 0.822–0.947, respectively. A higher R^2 value demonstrates that the model describes the adsorption kinetics better [7]. As shown in Table 4, the results revealed that the experimental data did not agree with the pseudo-first-order and Elovich kinetic models. The amounts of adsorption correlated well with the pseudo-second-order kinetics. Figs. 5–7 show the curve-fitting plots of the pseudo-first-order, pseudo-second-order,

Table 4
Comparison of the pseudo-first-order, pseudo-second-order and Elovich adsorption constants for Cr(VI)

Concentration of Cr(VI) (mg/L)	Pseudo-first-order			Pseudo-second-order			Elovich		
	K_1 ($\times 10^2$ min^{-1})	q_e (mg/g)	R^2	K_2 ($\times 10^2$ g/mg·min)	q_e (mg/g)	R^2	α	β	R^2
2	4.68	285.4	0.966	11.94	345.4	0.948	0.120	32.29	0.947
3	4.62	270.4	0.933	13.35	571.3	0.912	0.114	30.76	0.902
5	4.53	272.2	0.920	13.94	618.3	0.907	0.114	30.69	0.900
6	4.39	259.3	0.912	15.58	655.7	0.875	0.109	29.33	0.860
8	4.34	250.2	0.897	16.22	675.6	0.872	0.107	28.95	0.849
9	4.25	248.1	0.886	17.45	794.3	0.840	0.104	28.10	0.824
10	4.20	239.1	0.855	18.32	944.1	0.822	0.104	28.03	0.822

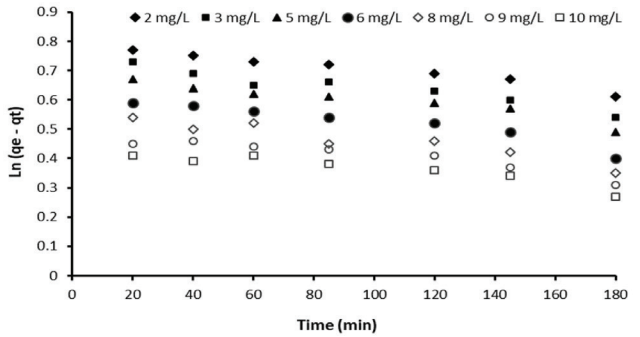

Fig. 5. Plots of adsorption first-order-kinetics for Cr(VI) on DSSS at concentrations of 2, 3, 5, 6, 8, 9 and 10 mg/L.

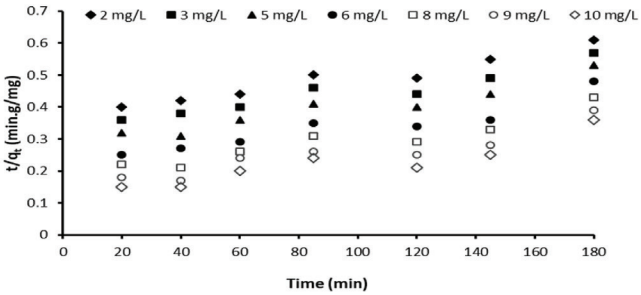

Fig. 6. Plots of adsorption second-order-kinetics for Cr(VI) on DSSS at concentrations of 2, 3, 5, 6, 8, 9 and 10 mg/L.

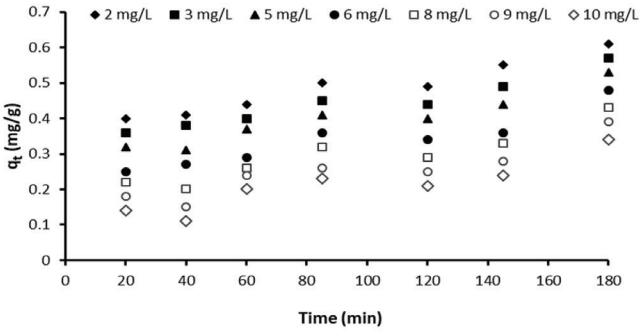

Fig. 7. Plots of adsorption Elovich kinetics for Cr(VI) on DSSS at concentrations of 2, 3, 5, 6, 8, 9 and 10 mg/L.

and Elovich kinetic models for Cr(VI) at concentrations of 2, 3, 5, 6, 8, 9 and 10 mg/L on DSSS. The kinetic modeling for the Cr(VI) adsorption kinetics on various adsorbents such as modified groundnut hull [49], activated carbon prepared from mango kernel [50], grafted banana peels [2], nano-onions [51] and pumice [52] was tested in different studies. Their results indicated a good fit of the experimental data with pseudo-second-order kinetic model compared to pseudo-first-order and other kinetic models.

3.4. Adsorption isotherms

As shown in Figs. 8–10, different isotherm models including the Langmuir, Freundlich, and Temkin models for Cr(VI) adsorption on DSSS were studied to determine which isotherm is more suitable. To achieve the parameters of the Langmuir isotherm shown in Table 5, we studied the plot of C_e/q_e against C_e. The maximum adsorption efficiency (q_m) of DSSS for Cr(VI) was identified to be 105.31 mg/g and the adsorption energy (K_l) value was identified to be 0.894 L/mg. The correlation coefficients (R^2) were applied to describe the conformity of the adsorption data to the studied isotherms. The Cr(VI) adsorption data are well-fitted to the Freundlich and Langmuir isotherms, (Figs. 8 and 9). The following order based on the results is the reason for the obedience of Cr(VI) adsorption on DSSS.

Cr(VI): Langmuir isotherm (R^2 = 0.97) > Freundlich isotherm (R^2 = 0.949) > Temkin isotherm (R^2 = 0.912).

The correlation coefficient of Freundlich isotherm model is lower than that of Langmuir isotherm model, as shown in Table 5. This demonstrates that Langmuir model fits the data better. This means that the adsorbate tends to be adsorbed on homogenous binding sites; it also reveals the monolayer coverage of adsorbate molecules at the homogeneous binding sites of the adsorbent surface [7]. The constants of the Freundlich adsorption model associated with the adsorption capacity and adsorption intensity are K_f and n, respectively. The plot of log (q_e) against log (C_e) computed the values of K_f and n, as shown in Fig. 10. In the Freundlich equilibrium, the value of K_f constant was shown to be 1.33 g/L. The "n" value shows that the

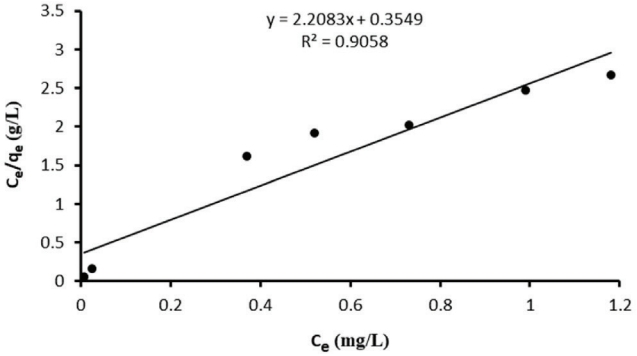

Fig. 8. Langmuir isotherm model of Cr(VI) onto DSSS.

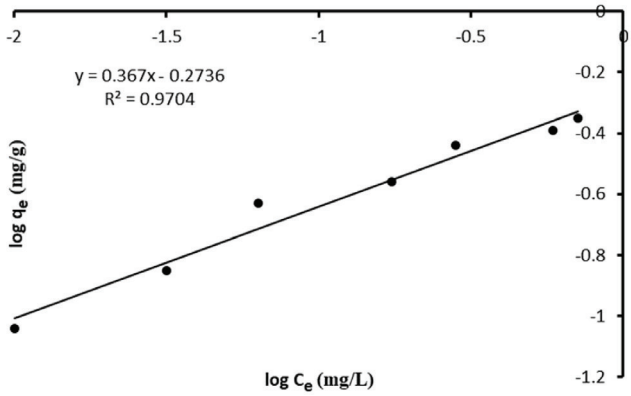

Fig. 9. Freundlich isotherm model of Cr(VI) onto DSSS.

Table 5
Parameters and correlation coefficient of Langmuir, Freundlich and Temkin for Cr(VI) adsorption

Langmuir model			Freundlich model			Temkin model		
K_L (L/mg)	q_m (mg/g)	R^2	K_f (g/(mg·min))	n	R^2	K_T	B	R^2
0.894	105.31	0.97	1.33	2.095	0.949	0.456	12.058	0.912

adsorbent is effective, the surface is heterogeneous, and the processes have a great affinity for metal ions. The high value of n indicates a strong bond between the adsorbent and the adsorbate and if $n > 1$, this indicates a favorable sorption process [52]. The observed n value was higher than 1.0, indicating the sorption of Cr(VI) onto DSSS and that is an agreeable process. The value of n was between 0 and 10, suggesting the relatively strong adsorption of Cr(VI) onto the surface of DSSS. In the present study, we found a value of 2.095 for n, but with lower correlation coefficients ($R^2 = 0.949$) this isotherm model was not the best model to illustrate these equilibria.

Similar results have been seen for the adsorption of Cr(VI) on various adsorbents [49–51]. And the results of some studies show good fits data for the adsorption of Cr(VI) with both the Langmuir and Freundlich isotherm models [2,52].

The plot of q_e against ln C_e determined the value of isotherm constant A and B from the slop and intercept, respectively, as seen in Fig. 10. The value of Temkin isotherm constants A and B was 0.456 and 12.058, respectively (Table 5). The correlation coefficient ($R^2 = 0.912$) for the adsorption of Cr(VI) in Temkin isotherm was the lowest fitness as compared to the two others isotherms.

3.5. Regeneration

Regeneration and recovery of the adsorbent are very important aspects in wastewater treatment processes and, therefore, desorption of chromium was tried with a number of eluents such as HNO_3, HCl, NH_4OH, and NaCl. It was found that the desorption of the metal ion occurred by 1% HNO_3. It was observed that the adsorbent loses about 3% capacity after the first run and about 10–15% after more than five runs. Therefore, the adsorbent can be used for at least five runs without any problem. It is very important to note here that DSSS is an easily available, inexpensive adsorbent, and its cost is very low in comparison to the cost of regeneration.

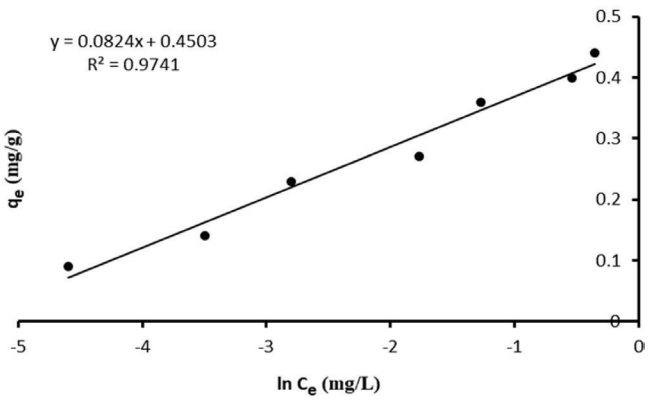

Fig. 10. Temkin isotherm model of Cr(VI) onto DSSS.

3.6. Comparison of Cr(VI) adsorption with different adsorbents

The adsorption capacity of the adsorbents for the adsorption of Cr(VI) was compared with those of others reported in the literature and the values of adsorption capacity, as presented in Table 6. The experimental data of the present investigation were compared with the reported values. Results of our investigation revealed that DSSS had a high adsorption capacity.

Table 6
Comparison of adsorption capacity of different adsorbents for the adsorption of Cr(VI)

Adsorbents	Adsorbent capacity (mg/g)	References
Wood apple shell	13.74	[53]
Ricinus communis seed shell active carbon	7.761	[54]
Palm shell activated carbon	12.6	[55]
PEI/palm shell activated carbon	20.5	[56]
Acid-modified waste activated carbon	10.93	[57]
Fe-modified bamboo carbon	35.7	[58]
Rice straw	3.15	[59]
Maize corn cob	0.28	[60]
Jatropha oil cake	0.82	[60]
Sugarcane bagasse	0.63	[60]
Sawdust	15.84	[61]
Olive cake	33.4	[61]
Pine needles	21.5	[61]
Almond	10.62	[61]
Coal	6.78	[62]
DSSS (dehydrated *Scrophularia striata* stems)	35.14	This study

4. Conclusions

Adsorption efficiency of Cr(VI) was investigated in the present study, using DSSS as a natural adsorbent. Lower initial Cr(VI) concentration led to higher adsorption efficiency. The adsorbent dosage of 2 g/100 mL generated the best result. Also, the adsorption efficiency of Cr(VI) in acidic (pH = 2) condition was high. The maximum adsorption efficiency of 94.3% was obtained for Cr(VI) at the reaction time of 180 min. Three models were used to describe the Cr(VI) adsorption kinetics. The kinetic data was shown to have the best fit with the pseudo-second-order model. Three isotherm models were used to the experimental equilibrium data. Based on the results, Langmuir isotherm had the best correlation for the adsorption of Cr(VI) onto DSSS. It is concluded that DSSS demonstrates interesting adsorption properties such as an efficient, economical adsorbent for adsorption of Cr(VI) from aqueous solutions.

Acknowledgments

The authors would like to thank the deputy of research and technology of Shiraz University of Medical Sciences for supporting the research project NO. 14528. The authors would like to thank the research-consulting center (RCC) for their assistance in editing this research article.

Symbols

R — The efficiency of Cr(VI) removal (%)
C_0 — The concentration of metal ions before adsorption (mg/L)
C_e — The concentration of metal ions after adsorption (mg/L)
q_e — The adsorption efficiency at equilibrium status (mg/g)
V — The volume of the aqueous phase (L)
M — The mass of the adsorbent (g)
q_t — The adsorption efficiency at t time (mg/g)
q_e — The adsorption efficiency at equilibrium (mg/g)
k_1 — The constant rate for pseudo-first-order model (L/min)
k_2 — The constant rate for pseudo-second-order model (g/mg·min)
α — The initial Cr(VI) concentration (mg/g·min)
β — The desorption constant (g/mg)
q_m — The maximum adsorption efficiency (mg/g)
K_L — Constant of Langmuir isotherm (L/mg)
K_f — Constant of Freundlich isotherm (L/mg)
n — Constant of Freundlich isotherm
K_T — The constant of Temkin isotherm (L/g)
B — The heat of adsorption (J/mol)
E_a — Activation energy (kJ/mol)
R_2 — Gas constant (kJ/mol.K)
T — Absolute temperature (K)
h — Planck constant ($\times 10^{-3}$ mg/g·min)
ΔS^* — Entropy of activation (kJ/mol·K)
ΔH^* — Enthalpy of activation (kJ/mol)
ΔG^* — Free energy of activation (kJ/mol)
EDX — Energy dispersive X-ray
SEM — Scanning electron microscope
FTIR — Fourier transform infrared

References

[1] M. Dehghani, M. Ansari Shiri, S. Shahsavani, N. Shamsedini, M. Nozari, Removal of Direct Red 81 dye from aqueous solution using neutral soil containing copper, Desal. Water. Treat., 86 (2017) 213–220.
[2] A. Ali, K. Saeed, F. Mabood, Removal of chromium (VI) from aqueous medium using chemically modified banana peels as efficient low-cost adsorbent, Alexandria. Eng. J., 55 (2016) 2933–2942.
[3] M. Ilyas, N. Khan, Q. Sultana, Thermodynamic and kinetic studies of chromium (VI) adsorption by sawdust activated carbon, J. Chem. Soc. Pak., 36 (2014) 1003–1012.
[4] Z.A. Al Othman, R. Ali, M. Naushad, Hexavalent chromium removal from aqueous medium by activated carbon prepared from peanut shell: adsorption kinetics, equilibrium and thermodynamic studies, Chem. Eng. J., 184 (2012) 238–247.
[5] E. Malkoc, Y. Nuhoglu, M. Dundar, Adsorption of chromium (VI) on pomace—an olive oil industry waste: batch and column studies, J. Hazard. Mater., 138 (2006) 142–151.
[6] C.C. Kan, A.H. Ibe, K.K.P. Rivera, R.O. Arazo, M.D.G. de Luna, Hexavalent chromium removal from aqueous solution by adsorbents synthesized from groundwater treatment residuals, Sustain. Environ. Res., 27 (2017) 163–171.
[7] M. Dehghani, M. Nozari, A. Fakhraei Fard, M. Ansari Shiri, N. Shamsedini, Direct Red 81 adsorption on iron filings from aqueous solutions; kinetic and isotherm studies, Environ. Technol., (2018) 1–28.
[8] M. Dehghani, Y. Kamali, F. Jamshidi, M. Ansari Shiri, M. Nozari, Contribution of H_2O_2 in ultrasonic systems for degradation of DR–81 dye from aqueous solutions, Desal. Water. Treat., 107 (2018) 332–339.
[9] N. Itankar, Y. Patil, Management of hexavalent chromium from industrial waste using low-cost waste biomass, Procedia. Soc. Behav. Sci., 133 (2014) 219–224.
[10] E. Oguz, Adsorption characteristics and the kinetics of the Cr(VI) on the Thuja oriantalis, Colloids. Surf. A. Physicochem. Eng. Asp., 252 (2005) 121–128.
[11] S.S. Baral, S.N. Das, P. Rath, Hexavalent chromium removal from aqueous solution by adsorption on treated sawdust, Biochem. Eng. J., 31 (2006) 216–222.
[12] M. Doltabadi, H. Alidadi, M. Davoudi, Comparative study of cationic and anionic dye removal from aqueous solutions using sawdust based adsorbent, Environ. Prog. Sustain. Energy., 35 (2016) 1078–1090.
[13] M. Rezaie Tavirani, S.A. Mortazavi, M. Barzegar, S.H. Moghadamnia, M.B. Rezaee, Study of anti cancer property of Scrophularia striata extract on the human astrocytoma cell line (1321), Iran. J. Pharm. Res., 9 (2010) 403–410.
[14] USEPA. pH USEPA 8156 electrode method. Hach Company: USA; 2015.
[15] R. Zhang, B. Wang, H. Ma, Studies on Chromium (VI) adsorption on sulfonated lignite, Desalination, 255 (2010) 61–66.
[16] R. Bennicelli, Z. Stępniewska, A. Banach, K. Szajnocha, J. Ostrowski, The ability of Azolla caroliniana to remove heavy metals (Hg (II), Cr (III), Cr (VI)) from municipal waste water, Chemosphere, 55 (2004) 141–146.
[17] N.K. Hamadi, X.D. Chen, M.M. Farid, M.G. Lu, Adsorption kinetics for the removal of chromium (VI) from aqueous solution by adsorbents derived from used tyres and sawdust, Chem. Eng. J., 84 (2001) 95–105.
[18] F. Gorzin, A.A. Ghoreyshi, Synthesis of a new low-cost activated carbon from activated sludge for the removal of Cr(VI) from aqueous solution: Equilibrium, kinetics, thermodynamics and desorption studies, Korean. J. Chem. Eng., 30 (2013) 1594–1602.
[19] M. Ghasemi, M. Naushad, N. Ghasemi, Y. Khosravi-Fard, Adsorption of Pb (II) from aqueous solution using new

adsorbents prepared from agricultural waste: adsorption isotherm and kinetic studies, J. Indus. Eng. Chem., 20 (2014) 2193–2199.
[20] K. Malwade, D. Lataye, V. Mhaisalkar, S. Kurwadkar, D. Ramirez, Adsorption of hexavalent chromium onto activated carbon derived from Leucaena leucocephala waste sawdust: kinetics, equilibrium and thermodynamics, Int. J. Environ. Sci. Technol., 13 (2016) 2107–2116.
[21] M. Naushad, T. Ahamad, B.M. Al-Maswari, A.A. Alqadami, S.M. Alshehri, Nickel ferrite bearing nitrogen-doped mesoporous carbon as efficient adsorbent for the removal of highly toxic metal ion from aqueous medium, Chem. Eng. J., 330 (2017) 1351–1360.
[22] M. Naushad, Surfactant assisted nano-composite cation exchanger: Development, characterization and applications for the removal of toxic Pb^{2+} from aqueous medium, Chem. Eng. J., 235 (2014) 100–108.
[23] M. Ghasemi, M. Naushad, N. Ghasemi, Y. Khosravi-Fard, A novel agricultural waste based adsorbent for the removal of Pb(II) from aqueous solution: kinetics, equilibrium and thermodynamic studies, J. Ind. Eng. Chem., 20 (2014) 454–461.
[24] Z.A. ALOthman, M. Naushad, R. Ali, Kinetic, equilibrium isotherm and thermodynamic studies of Cr(VI) adsorption onto low-cost adsorbent developed from peanut shell activated with phosphoric acid, Environ. Sci. Pollut. Res., 20 (2013) 3351–3365.
[25] T. Anirudhan, P. Radhakrishnan, Thermodynamics and kinetics of adsorption of Cu(II) from aqueous solutions onto a new cation exchanger derived from tamarind fruit shell, J. Chem. Thermodyn., 40 (2008) 702–709.
[26] S. Chowdhury, P. Saha, Adsorption thermodynamics and kinetics of malachite green onto Ca (OH) 2-treated fly ash, J. Environ. Eng., 137 (2010) 388–397.
[27] E.K. Silva, R.V. de Barros Fernandes, S.V. Borges, D.A. Botrel, F. Queiroz, Water adsorption in rosemary essential oil microparticles: Kinetics, thermodynamics and storage conditions, J. Food. Eng., 140 (2014) 39–45.
[28] J. Yang, M. Yu, T. Qiu, Adsorption thermodynamics and kinetics of Cr (VI) on KIP210 resin, J. Ind. Eng. Chem., 20 (2014) 480–486.
[29] R. Han, W. Zou, Z. Zhang, J. Shi, J. Yang, Removal of copper (II) and lead (II) from aqueous solution by manganese oxide coated sand: I. Characterization and kinetic study, J. Hazard. Mater., 137 (2006) 384–395.
[30] M. Chairat, S. Rattanaphani, J.B. Bremner, V. Rattanaphani, Adsorption kinetic study of lac dyeing on cotton, Dyes Pigm., 76 (2008) 435–439.
[31] D. Mohan, K.P. Singh, Single- and multi-component adsorption of cadmium and zinc using activated carbon derived from bagasse—an agricultural waste, Water Res., 36 (2002) 2304–2318.
[32] G. Sharma, D. Pathania, M. Naushad, Preparation, characterization, and ion exchange behavior of nanocomposite polyaniline zirconium (IV) selenotungstophosphate for the separation of toxic metal ions, Ionics, 21 (2015) 1045–1055.
[33] L. Levankumar, V. Muthukumaran, M. Gobinath, Batch adsorption and kinetics of chromium (VI) removal from aqueous solutions by Ocimum americanum L. seed pods, J. Hazard. Mater., 161 (2009) 709–713.
[34] M. Bansal, D. Singh, V. Garg, A comparative study for the removal of hexavalent chromium from aqueous solution by agriculture wastes' carbons, J. Hazard. Mater., 171 (2009) 83–92.
[35] A.K. Giri, R. Patel, S. Mandal, Removal of Cr (VI) from aqueous solution by Eichhornia crassipes root biomass–derived activated carbon, Chem. Eng. J., 185 (2012) 71–81.
[36] K.M. Doke, E.M. Khan, Equilibrium, kinetic and diffusion mechanism of Cr (VI) adsorption onto activated carbon derived from wood apple shell, Arabian. J. Chem., 10 (2017) 252–260.
[37] M.H. Dehghani, D. Sanaei, I. Ali, A. Bhatnagar, Removal of chromium (VI) from aqueous solution using treated waste newspaper as a low-cost adsorbent: Kinetic modeling and isotherm studies, J. Mol. Liq., 215 (2016) 671–679.
[38] M. Dehghani, S. Nasseri, S. Amin, Z. Zamanian, Assessment of atrazine distribution in Shiraz soils, south of Iran, Pak. J. Biol. Sci., 13 (2010) 66–72.
[39] A. Shukla, Y.H. Zhang, P. Dubey, J. Margrave, S.S. Shukla, The role of sawdust in the removal of unwanted materials from water, J. Hazard. Mater., 95 (2002) 137–152.
[40] M. Dehghani, S. Nasseri, H. Hashemi, Study of the bioremediation of atrazine under variable carbon and nitrogen sources by mixed bacterial consortium isolated from corn field soil in Fars province of Iran, J. Environ. Public. Health, 2013 (2013) 1–7.
[41] A.B. Albadarin, C. Mangwandi, H. Ala'a, G.M. Walker, S.J. Allen, M.N. Ahmad, Kinetic and thermodynamics of chromium ions adsorption onto low-cost dolomite adsorbent, Chem. Eng. J., 179 (2012) 193–202.
[42] M.Y. Arıca, G. Bayramoğlu, M. Yılmaz, S. Bektaş, Ö. Genç, Biosorption of Hg^{2+}, Cd^{2+}, and Zn^{2+} by Ca-alginate and immobilized wood-rotting fungus Funalia trogii, J. Hazard. Mater., 109 (2004) 191–199.
[43] L. Rafati, A. Mahvi, A. Asgari, S. Hosseini, Removal of chromium (VI) from aqueous solutions using Lewatit FO36 nano ion exchange resin, Int. J. Environ. Sci. Technol., 7 (2010) 147–156.
[44] N. Saifuddin, A. Raziah, Removal of heavy metals from industrial effluent using Saccharomyces cerevisiae (Baker's yeast) immobilized in chitosan/lignosulphonate matrix, J. Appl. Sci. Res., 3 (2007) 2091–2099.
[45] A. Bhattacharya, T. Naiya, S. Mandal, S. Das, Adsorption, kinetics and equilibrium studies on removal of Cr (VI) from aqueous solutions using different low-cost adsorbents, Chem. Eng. J., 137 (2008) 529–541.
[46] A.I. Zouboulis, N.K. Lazaridis, K.A. Matis, Removal of toxic metal ions from aqueous systems by biosorptive flotation, J. Chem. Technol. Biotechnol., 77 (2002) 958–964.
[47] F.-S. Zhang, J.O. Nriagu, H. Itoh, Photocatalytic removal and recovery of mercury from water using TiO_2-modified sewage sludge carbon, J. Photochem. Photobiol. A. Chem., 167 (2004) 223–228.
[48] M.F. Yardim, T. Budinova, E. Ekinci, N. Petrov, M. Razvigorova, V. Minkova, Removal of mercury (II) from aqueous solution by activated carbon obtained from furfural, Chemosphere, 52 (2003) 835–841.
[49] S.O. Owalude, A.C. Tella, Removal of hexavalent chromium from aqueous solutions by adsorption on modified groundnut hull, Beni-suef. Univ. J. Basic. Appl. Sci., 5 (2016) 377–388.
[50] M.K. Rai, G. Shahi, V. Meena, S. Chakraborty, R.S. Singh, B.N. Rai, Removal of hexavalent chromium Cr (VI) using activated carbon prepared from mango kernel activated with H_3PO_4, Resour. Effic. Technol., 2 (2016) 63–70.
[51] C. Sakulthaew, C. Chokejaroenrat, A. Poapolathep, T. Satapanajaru, S. Poapolathep, Hexavalent chromium adsorption from aqueous solution using carbon nano-onions (CNOs), Chemosphere, 184 (2017) 1168–1174.
[52] C.W. Muriuki, U.N. Mutwiwa, P.G. Home, F.N. Kilonzo, Adsorption of hexavalent chromium from aqueous solution by pumice: equilibrium and kinetic study, Proc. Sustainable. Res. Innov. Conf., 5 (2014) 209–214.
[53] A.S. Sartape, P.D. Raut, S.S. Kolekar, Efficient adsorption of chromium (VI) ions from aqueous solution onto a low-cost adsorbent developed from limonia acidissima (wood apple) shell, Adsorpt. Sci. Technol., 28 (2010) 547–560.
[54] P. Thamilarasu, K. Karunakaran, Kinetic, equilibrium and thermodynamic studies on removal of Cr (VI) by activated carbon prepared from Ricinus communis seed shell, Can. J. Chem. Eng., 91 (2013) 9–18.
[55] B.K. Hamad, A.M. Noor, A.A. Rahim, Removal of 4-chloro-2-methoxyphenol from aqueous solution by adsorption to oil palm shell activated carbon activated with K_2CO_3, J. Phys. Sci., 22 (2011) 39–55.
[56] M. Owlad, M.K. Aroua, W.M.A.W. Daud, Hexavalent chromium adsorption on impregnated palm shell activated carbon with polyethyleneimine, Bioresour. Technol., 101 (2010) 5098–5103.

[57] P.K. Ghosh, Hexavalent chromium [Cr (VI)] removal by acid modified waste activated carbons, J. Hazard. Mater., 171 (2009) 116–122.
[58] W. Wang, X. Wang, X. Wang, L. Yang, Zh. Wu, Si. Xia, Ji. Zhao, Cr (VI) removal from aqueous solution with bamboo charcoal chemically modified by iron and cobalt with the assistance of microwave, J. Environ. Sci., 25 (2013) 1726–1735.
[59] H. Gao, Y. Liu, G. Zeng, W. Xu, T. Li, W. Xia, Characterization of Cr (VI) removal from aqueous solutions by a surplus agricultural waste—rice straw, J. Hazard. Mater., 150 (2008) 446–452.
[60] U.K. Garg, M. Kaur, V. Garg, D. Sud, Removal of hexavalent chromium from aqueous solution by agricultural waste biomass, J. Hazard. Mater., 140 (2007) 60–68.
[61] M. Dakiky, M. Khamis, A. Manassra, M. Mer'Eb, Selective adsorption of chromium (VI) in industrial wastewater using low-cost abundantly available adsorbents, Adv. Environ. Res., 6 (2002) 533–540.
[62] V. Gupta, S. Srivastava, D. Mohan, S. Sharma, Design parameters for fixed bed reactors of activated carbon developed from fertilizer waste for the removal of some heavy metal ions, Waste. Manage., 17 (1998) 517–522.